Unit Commitment With Gas Network Awareness

Geunyeong Byeon and Pascal Van Hentenryck, Member, IEEE

Abstract—Recent changes in the fuel mix for electricity generation and, in particular, the increase in Gas-Fueled Power Plants (GFPP), have created significant interdependencies between the electrical power and natural gas transmission systems. However, despite their physical and economic couplings, these networks are still operated independently, with asynchronous market mechanisms. This mode of operation may lead to significant economic and reliability risks in congested environments as revealed by the 2014 polar vortex event experienced by the northeastern United States. To mitigate these risks, while preserving the current structure of the markets, this paper explores the idea of introducing gas network awareness into the standard unit commitment model. Under the assumption that the power system operator has some (or full) knowledge of gas demand forecast and the gas network, the paper proposes a tri-level mathematical program where natural gas zonal prices are given by the dual solutions of natural-gas flux conservation constraints and commitment decisions are subject to bid-validity constraints that ensure the economic viability of the committed GFPPs. This tri-level program can be reformulated as a single-level Mixed-Integer Second-Order Cone program which can then be solved using a dedicated Benders decomposition. The approach is validated on a case study for the Northeastern United States [1] that can reproduce the gas and electricity price spikes experienced during the early winter of 2014. The results on the case study demonstrate that gas awareness in unit commitment is instrumental in avoiding the peaks in electricity prices while keeping the gas prices to reasonable levels.

Index Terms—Unit commitment, multi-energy systems, hierarchical optimization, interdependencies, polar vortex.

I. INTRODUCTION

AS-Fueled Power Plants (GFPPs) have become a significant part of the energy mix in the last decades, primarily because of their operational flexibility and lower environmental impacts. Although GFPPs have introduced interdependencies between the natural gas and electrical power systems, these networks are still operated independently, with asynchronous market mechanisms. In particular, the unit commitment decisions in the electrical power system take place before the

Manuscript received February 11, 2019; revised April 26, 2019, June 1, 2019, and August 5, 2019; accepted September 5, 2019. Date of publication September 19, 2019; date of current version February 26, 2020. This work was partly supported by an NSF CRISP Award (NSF-1638331) "Computable Market and System Equilibrium Models for Coupled Infrastructures." Paper no. TPWRS-00205-2019. (Corresponding author: Geunyeong Byeon.)

- G. Byeon is with the Department of Industrial and Operations Engineering, University of Michigan, Ann Arbor, MI 48109 USA (e-mail: gbyeon@umich.edu).
- P. V. Hentenryck is with the H. Milton Stewart School of Industrial and Systems Engineering, Georgia Institute of Technology, Atlanta, GA 30332 USA (e-mail: pvh@isye.gatech.edu).

Color versions of one or more of the figures in this article are available online at http://ieeexplore.ieee.org.

This article has supplementary downloadable material available at http://ieeexplore.ieee.org, provided by the authors.

Digital Object Identifier 10.1109/TPWRS.2019.2942298

realization of natural gas spot prices, introducing reliability risks and economic inefficiencies in congested environments. Indeed, the GFPPs may not be able to secure gas at reasonable prices, introducing either reliability issues or electricity price spikes.

This undesirable outcome occurred in the Northeastern United States during the early winter of 2014. Extremely low temperatures induced an unusual coincident peak in electricity and natural gas demand. On the one hand, it produced record-high natural gas spot prices due to congestion. On the other hand, high electricity loads led the electrical power system operator to call for some emergency actions, which resulted in higher electricity prices [2]. Moreover, the power system operator, valuing reliability the most, encouraged committed GFPPs to buy natural gas at all costs without assurance of cost recovery, further aggravating the economic cost [3]. It is important to mention that the critical issue in this case was not the gas supply, but rather congestion in the gas transmission network. Moreover, a recent study [1] has shown that the cost of expanding the gas and electricity network infrastructure to avoid such events would be prohibitive.

To address these interdependencies, a number of researchers have studied how to incorporate the natural gas transmission capabilities into the operational decisions of electrical power systems. See, for instance, [4]–[13]. Other researchers have also studied how to incorporate the economic coupling between these two infrastructure systems using new market mechanisms. A new market framework with a joint ISO, using price- or volume-based approaches, was investigated in [14], [15]. Instead of introducing one joint ISO, other researchers have proposed a new market framework that assumes centralized independent gas markets, synchronizes the electricity and gas market days, and allows some information exchange between some parties in the electricity and gas markets (e.g., market operators or GFPPs) [16]–[21].

This paper takes a different approach that stays within the current operating practices and does not introduce a new market mechanism. Instead, the approach generalizes the unit commitment model to capture the physical and economic couplings and strive to ensure both physical feasibility and economic viability of GFPPs. More precisely, the paper introduces the Unit Commitment problem with Gas Network Awareness (UCGNA) to schedule a set of generating units for the next day while taking account the fuel delivery and the natural gas prices that are propagated back by the natural gas system. The UCGNA imposes bid-validity constraints on the GFPPs to ensure their profitability and estimates the natural gas prices for these constraints with the dual solutions associated with the flux conservation constraints of the gas market.

The UCGNA is formulated as a tri-level mathematical program and assumes that the power system operator has partial (or full) knowledge on gas demand forecast and gas network. When the power system is modeled with its DC approximation and the gas network with the second-order cone program from [22] to model its steady-state physics, the tri-level mathematical program can be reformulated as a single-level Mixed-Integer Second-Order Cone Program (MISOCP) through strong duality of the innermost problem. The resulting MISOCP can then be solved using a dedicated Benders decomposition recently proposed in [23].

The key contributions of this paper are threefold. First, it proposes the first unit commitment model (UCGNA) that incorporates both the physical and economic couplings of electrical power and natural gas transmission systems and can be used within current operating practices. Second, it proposes a MISOCP that captures the UCGNA and can be solved through Benders decomposition. Finally, it demonstrates the potential practicality of the approach on a detailed case study that replicates the behavior of the 2014 polar vortex event on the Northeastern United States. In particular, the paper shows that, on the case study, the UCGNA obtains a functional unit commitment decision, which avoids the electricity price peaks and keeps the total gas costs reasonable, contrary to current practice, even for highly congested electrical and gas networks.

The rest of this paper is organized as follows. Section II formalizes the UCGNA and Section III presents the MISOCP. Section IV briefly reviews the solution methods for the MISOCP. Section V describes the test cases and Section VI analyzes the behavior of the model on the case study. Lastly, Section VII discusses implications of the UCGNA and Section VIII concludes the paper.

II. UNIT COMMITMENT WITH GAS AWARENESS

This section specifies the UCGNA, including its electricity system, its natural gas network, and their physical and economic couplings. The electricity transmission grid is represented by an undirected graph $\mathcal{G}^e = (\mathcal{N}, \mathcal{E})$ and the natural gas transmission system by a directed graph $\mathcal{G}^g = (\mathcal{V}, \mathcal{A})^1$. Boldface letters represent vectors of variables, $[a,b]_{\mathbb{Z}}$ denotes the set of integers in interval [a,b], and [n] denotes the set $\{1,\ldots,n\}$ for some integer $n \geq 1$. The letter \mathcal{T} denotes the set of time periods $\{0,1,\ldots,T\}$.

A. The Electricity Transmission System

In the United States, Unit Commitment (UC) and Economic Dispatch (ED) problems are solved daily to determine the hourly operating schedule of generating units for the next day from bids submitted by market participants. Tables I and II summarize the parameters and variables of the UC/ED problems. With these notations, the UC model is specified in Problem (1).

TABLE I PARAMETERS OF THE ELECTRICITY SYSTEM

$\mathcal{G}^e = (\mathcal{N}, \mathcal{E})$	Undirected graph where \mathcal{N} is a set of buses indexed by $i=1,\cdots,N$ and \mathcal{E} is a set of lines
	indexed with $l = 1, \cdots, E$
\mathcal{U}	Set of generators, indexed by $u = 1, \dots, U$
$\mathcal{U}^g\subseteq\mathcal{U}$	Set of GFPPs
\mathcal{U} $\mathcal{U}^g \subseteq \mathcal{U}$ $\mathcal{U}(i) \subseteq \mathcal{U}$	Set of generators located at $i \in \mathcal{N}$
\mathcal{B}_u	Set of supply bids submitted by $u \in \mathcal{U}$, indexed
w.	by $b=1,\cdots,B_u$
β_{b}	Bid price of $b \in \mathcal{B}_u$
$\frac{1}{S}h$	Amount of real power generation of $b \in \mathcal{B}_u$
$\frac{\beta_b}{\overline{s}_b} \\ \underline{p}_u, \overline{p}_u$	Minimum/maximum real power generation of
	$u \in \mathcal{U}$
$\frac{R}{c_u}$, \overline{R}_u	Ramp-down/-up rate of $u \in \mathcal{U}$
$\frac{\underline{r}_u}{c}$	No-load cost of $u \in \mathcal{U}$
Ψ_u	Set of counts of time periods with distinct start-up
± u	costs of u indexed by h
$C_{u,h}$	Start-up cost of $u \in \mathcal{U}$ when u is turned on after it
,	has been offline for some time $\in [\Psi_{u,h}, \Psi_{u,h+1}]$
$\overline{o}_{u,0}, \overline{p}_{u,0}$	Initial on-off status/real power generation of $u \in$
-,-,1 4,0	\mathcal{U}
$\underline{\tau}_u, \overline{\tau}_{\underline{u}}$	Minimum-down/-up time of $u \in \mathcal{U}$
$\underline{\underline{\tau}}_{u,0}, \underline{\overline{\tau}}_{u,0}$	The time that generator $u \in \mathcal{U}$ has to be inac-
	tive/active from $t = 0$
$\frac{b_l}{f_l} \atop (d_{i,t}^e)_{i \in \mathcal{N}} \atop \Delta_l}$	Line susceptance of $l \in \mathcal{E}$
\overline{f}_1	Real power limit of $l \in \mathcal{E}$
$(d_{i+1}^e)_{i\in\mathcal{N}}$	Electricity load profile during $t \in \mathcal{T}$
Δ_l	Maximum voltage angle difference between two
•	end-points of $l \in \mathcal{E}$
$\underline{\theta}_i, \overline{\theta}_i$	Minimum/maximum voltage angle at $i \in \mathcal{N}$
-1, - 0	

TABLE II VARIABLES OF THE ELECTRICITY SYSTEM

Binary variables

 $o_{u,t}$ 1 if $u \in \mathcal{U}$ is on during $t \in \mathcal{T}$, 0 otherwise

 $v_{u,t}^+$ 1 if $u \in \mathcal{U}$ becomes online during $t \in \mathcal{T}$, 0 otherwise

 $v_{u,t}^{-}$ 1 if $u \in \mathcal{U}$ becomes offline during $t \in \mathcal{T}$, 0 otherwise

Continuous variables

 $s_{b,t}^e$ Real power generation from $b \in \mathcal{B}_u$ of $u \in \mathcal{U}$ during $t \in \mathcal{T}$

 $\begin{array}{ll} p_{u,t} & \text{Real power generation of } u \in \mathcal{U} \text{ during } t \in \mathcal{T} \\ f_{l,t} & \text{Real power flow on } l \in \mathcal{E} \text{ during } t \in \mathcal{T} \end{array}$

 $\begin{array}{ll} f_{l,t} & \text{Rear power flow off } t \in \mathcal{E} \text{ during } t \in \mathcal{T} \\ r_{u,t} & \text{Start-up cost of } u \in \mathcal{U} \text{ during } t \in \mathcal{T} \\ \theta_{i,t} & \text{Voltage angle on } i \in \mathcal{N} \text{ during } t \in \mathcal{T} \\ \end{array}$

$$\min \sum_{t \in [T]} \sum_{u \in \mathcal{U}} (c_u o_{u,t} + r_{u,t} + \sum_{b \in \mathcal{B}_u} \beta_b s_{b,t}^e)$$
 (1a)

s.t.
$$r_{u,t} \ge C_{u,h}(o_{u,t} - \sum_{n \in [h]} o_{u,t-n}),$$

$$\forall h \in \Psi_s, u \in \mathcal{U}, t \in [T], \tag{1b}$$

$$r_{u,t} \ge 0, \ \forall u \in \mathcal{U}, t \in [T],$$
 (1c)

$$o_{u,t} = \overline{o}_{u,0}, \ \forall u \in \mathcal{U}, \ t \in [0, \overline{\tau}_{u,0} + \underline{\tau}_{u,0}]_{\mathbb{Z}},$$
 (1d)

$$\sum_{t' \in [t - \overline{\tau}_u + 1, t]_{\mathbb{Z}}} v_{u, t'}^+ \le o_{u, t},$$

$$\forall u \in \mathcal{U}, \ t \in [\max{\{\overline{\tau}_u, \overline{\tau}_{u,0} + 1\}}, T]_{\mathbb{Z}},$$
 (1e)

$$\sum_{t' \in [t-\underline{\tau}_u+1,t]_{\mathbb{Z}}} v_{u,t'}^+ \leq 1 - o_{u,t-\underline{\tau}_u},$$

$$\forall u \in \mathcal{U}, \ t \in [\max\{\underline{\tau}_u, \underline{\tau}_{u,0} + 1\}, T]_{\mathbb{Z}}, \tag{1f}$$

¹In this paper, the gas flux direction is assumed to be fixed, since many modern gas networks are not as loopy as the power transmission systems, and they are nearly tree like [24]. Therefore, for most of the pipelines, the flow directions remain unchanged. In addition, since the changes in natural gas flux are in a much slower pace, the directions do not vary too much from day to another. For a non-tree like network, we can generalize the model by including binary variables that represent the flux direction [22].

$$v_{u,t}^+ - v_{u,t}^- = o_{u,t} - o_{u,t-1}, \forall u \in \mathcal{U}, \ t \in [T],$$
 (1g)

$$v_{u,t}^+, v_{u,t}^-, o_{u,t} \in \{0,1\}, \forall u \in \mathcal{U}, \ t \in [T],$$
 (1h)

$$s^e = \operatorname{argmin} \mathcal{Q}(o, v^+, v^-), \tag{1i}$$

where $Q(u, v^+, v^-)$ denotes the ED problem specified as follows:

$$\min \sum_{t \in [T]} \sum_{u \in \mathcal{U}} \left(\sum_{b \in \mathcal{B}_u} \beta_b s_{b,t}^e \right) \tag{1j}$$

$$\text{s.t.} \sum_{u \in \mathcal{U}(i)} p_{u,t} - d_{i,t}^e = \sum_{l \in \mathcal{E}: l_t = i} f_{l,t} - \sum_{l \in \mathcal{E}: l_h = i} f_{l,t},$$

$$\forall i \in \mathcal{N}, \ t \in [T], \tag{1k}$$

$$p_{u,t} = \sum_{b \in \mathcal{B}_u} s_{b,t}^e \, \forall u \in \mathcal{U}, \ t \in [T], \tag{11}$$

$$0 \le s_{b,t}^e \le \overline{s}_b, \ \forall b \in \mathcal{B}_u, \ u \in \mathcal{U}, \ t \in [T], \tag{1m}$$

$$p_u o_{u,t} \le p_{u,t} \le \overline{p}_u o_{u,t}, \ \forall u \in \mathcal{U}, \ t \in [T], \tag{1n}$$

$$p_{u,0} = \overline{p}_{u,0}, \ \forall u \in \mathcal{U}, \tag{10}$$

$$p_{u,t} - p_{u,t-1} \le \overline{R}_u o_{u,t-1} + \overline{p}_u v_{u,t}^+, \ \forall u \in \mathcal{U}, \ t \in [T],$$

$$(1p)$$

$$p_{u,t-1} - p_{u,t} \le \underline{R}_u o_{u,t-1} + \underline{p}_u v_{u,t}^-, \ \forall u \in \mathcal{U}, \ t \in [T],$$
(1q)

$$f_{l,t} = -b_l(\theta_{l_h,t} - \theta_{l_t,t}), \ \forall l \in \mathcal{E}, \ t \in [T], \tag{1r}$$

$$-\overline{f}_{l} \le f_{l,t} \le \overline{f}_{l}, \ \forall l \in \mathcal{E}, \ t \in [T], \tag{1s}$$

$$\underline{\theta}_i \le \theta_{i,t} \le \overline{\theta}_i, \ \forall i \in \mathcal{N}, \ t \in [T],$$
 (1t)

$$-\Delta_{l} < \theta_{l, t} - \theta_{l, t} < \Delta_{l}, \forall l \in \mathcal{E}, t \in [T]. \tag{1u}$$

The objective function of the upper level problem (Equations (1a)–(1h)) includes the no-load costs, the start-up costs, and the costs of the selected supply bids of each electrical power generating units. Equation (1b) computes the start-up cost $r_{u,t}$ of a generator u for time period t based on how long u has been offline [25]. The expression $o_{u,t} - \sum_{n=1}^h o_{u,t-n}$ is one when generator u becomes online after it has been turned off for h time periods. Equation (1c) states the nonnegativity requirement on $r_{u,t}$. Equation (1d) specifies the initial on-off status of each generator. The minimum-up and -down constraints are specified in Equations (1e) and (1f) respectively. The relationship between the variables for the on-off, start-up, and shut-down statuses of each generator is stated in Equation (1g). The binary requirements for logical variables $v_{u,t}^+, v_{u,t}^-, o_{u,t}$ are specified in Equation (1h).

Based on the commitment decisions, the lower-level problem (i.e., Equations (1j)–(1u)) decides the hourly operating schedule of each committed generators in order to minimize the system production costs. Equation (1k) states the flow conservation constraints for real power at each bus, using l_h and l_t to represent the head and tail of $l \in \mathcal{E}$. Equation (1l) states that the total real power generation of a generator u is equal to the production of its selected bids. Equation (1m) constrains the power generation

TABLE III
PARAMETERS OF THE GAS SYSTEM

$\mathcal{G}^g = (\mathcal{V}, \mathcal{A})$	Directed graph representing a natural gas transmission network, where \mathcal{V} is a set of junctions, indexed with $j=1,\cdots,V$, and $\mathcal{A}\subseteq\mathcal{V}\times\mathcal{V}$ is a
	set of connections, indexed with $a = 1, \dots, A$
$\mathcal{A}_c\subseteq\mathcal{A}$	Set of compressors
$\mathcal{A}_v \mathrel{\overline{\subseteq}} \mathcal{A}$	Set of control valves
κ_j	Cost of demand shedding at $j \in \mathcal{V}$
$(d_{j,t}^g)_{j\in\mathcal{V}}$	Gas demand profile during $t \in \mathcal{T}$
$(\overset{\circ}{d}_{j,\underline{t}}^g)_{j\in\mathcal{V}}\ \underline{s}_j^g,\overline{s}_j^g$	Lower/Upper limit on natural gas supply at $j \in \mathcal{V}$
$c_j(\cdot)$	Cost function for gas supply at $j \in \mathcal{V}$
W_a	Pipeline resistance (Weymouth) factor of $a \in A$
$\frac{\underline{\pi}_j}{\underline{\alpha}_a^c}, \overline{\overline{\alpha}_a^c} \\ \underline{\underline{\alpha}_a^c}, \overline{\overline{\alpha}_a^c}$	Minimum/maximum squared pressure at $j \in \mathcal{V}$
$\underline{\alpha}_{a}^{c}, \overline{\alpha}_{a}^{c}$	Lower/upper compression ratio of $a \in A_c$
$\underline{\alpha}_a^{\overline{v}}, \overline{\alpha}_a^{\overline{v}}$	Lower/upper control ratio of $a \in \mathcal{A}_v$

 $s_{b,t}^e$ from bid $b \in \mathcal{B}_u$ to be no more than the submitted amount \bar{s}_b . Equation (1n) enforces the bound on the real power generation of each generator. Equation (1o) specifies the initial generation amount of each generator, and Equations (1p) and (1q) state the ramp-up and -down constraints of each generator. Equation (1r) captures the DC approximation of the power flow equations and Equation (1s) specifies the thermal limit on each line. Equations (1t) and (1u) state the voltage angle bounds on each bus and the bounds on the angle difference of two adjacent buses respectively.

B. The Natural Gas Transmission System

$$\min \sum_{t \in [T]} \sum_{j \in \mathcal{V}} \left(\sum_{s \in \mathcal{S}_j} c_{j,s} s_{s,t}^g + \kappa_j q_{j,t} \right)$$
(2a)

$$\text{s.t. } s_{j,t}^g - l_{j,t} - \gamma_{j,t} = \sum_{a \in \mathcal{A}: a_t = j} \phi_{a,t} - \sum_{a \in \mathcal{A}: a_h = j} \phi_{a,t},$$

$$\forall j \in \mathcal{V}, t \in [T],\tag{2b}$$

$$l_{i,t} = d_{i,t}^g - q_{i,t}, \forall j \in \mathcal{V}, t \in [T], \tag{2c}$$

$$0 \le q_{i,t} \le d_{i,t}^g, \forall j \in \mathcal{V}, t \in [T], \tag{2d}$$

$$\phi_{a,t} \ge 0, \forall a \in \mathcal{A}, t \in [T],$$
 (2e)

$$\underline{s}_{i}^{g} \le s_{i,t}^{g} \le \overline{s}_{i}^{g}, \forall j \in \mathcal{V}, \ t \in [T], \tag{2f}$$

$$\underline{\alpha}_{a}^{c} \pi_{a_{h}, t} \leq \pi_{a_{t}, t} \leq \overline{\alpha}_{a}^{c} \pi_{a_{h}, t}, \forall a \in \mathcal{A}_{c}, \ t \in [T], \tag{2g}$$

$$\underline{\alpha}_{a}^{v} \pi_{a_{h}, t} \leq \pi_{a_{t}, t} \leq \overline{\alpha}_{a}^{v} \pi_{a_{h}, t}, \forall a \in \mathcal{A}_{v}, \ t \in [T], \tag{2h}$$

$$\pi_{a_h,t} - \pi_{a_t,t} = W_a \phi_{a,t}^2, \forall a \in \mathcal{A} \setminus (\mathcal{A}_v \cup \mathcal{A}_c), \ t \in [T],$$
(2i)

$$\underline{\pi}_i \le \pi_{i,t} \le \overline{\pi}_i, \forall j \in \mathcal{V}, \ t \in [T]$$
 (2j)

$$s_{j,t}^g = \sum_{s \in S_i} s_{s,t}^g \tag{2k}$$

Tables III and IV specify the parameters and variables of the steady-state natural gas model, which is given in Problem (2). The modeling is similar to those in [1], [22], [26] and uses the Weymouth equation to capture the relationship between pressures and flux. The flux conservation constraint is given

TABLE IV VARIABLES OF THE GAS SYSTEM

$s_{k,t}^{g}$	Amount of gas supplied by $k \in \mathcal{K}$ during $t \in \mathcal{I}$
$\pi_{j,t}$	Pressure squared at $j \in \mathcal{V}$ during $t \in \mathcal{T}$
$\phi_{a,t}$	Gas flow on $a \in \mathcal{A}$ during $t \in \mathcal{T}$
$l_{i,t}$	Satisfied gas demand at $j \in \mathcal{V}$ during $t \in \mathcal{T}$
$q_{i,t}$	Amount of gas demand shedding at $j \in \mathcal{V}$ during $t \in \mathcal{T}$
$\gamma_{j,t}$	Total amount of gas consumed by the GFPP located at $j \in$
	$\mathcal{N} \cap \mathcal{V}$ during $t \in \mathcal{T}$

TABLE V
PARAMETERS FOR THE ELECTRICITY AND GAS COUPLING

$\{H_{u,i}\}_{i=0,1,2}$	Coefficients of the heat rate curve of $u \in \mathcal{U}^g$
α_u	Maximum allowable percentage of the expense on
	natural gas over its marginal bid price for $u \in \mathcal{U}^g$
\mathcal{K}	Set of pricing zones, indexed with $k = 1, \dots, K$
$\mathcal{V}(k)$	Set of junctions that belong to $k \in \mathcal{K}$

in Equation (2b), where a_h and a_t represent the head and tail of $a \in A$. Equation (2c) determines the demand served at each junction: It captures the amount of gas load shedding which must be nonnegative and cannot exceed the demand at the corresponding junction (Equation (2d)). The model assumes that gas flow directions are predetermined and Equation (2e) enforces the sign of gas flow variables, i.e., it constrains $\phi_{a,t}$ to be nonnegative. Equation (2f) specifies the upper and lower limits of natural gas supplies. The change in pressure through compressors and control valves are formulated in Equations (2g) and (2h) and the model uses a single compressor machine approximation as in prior work. The steady-state physics of gas flows is formulated with the Weymouth equation in Equation (2i). Equation (2j) states the bounds on nodal pressures. Equation (2i) can be convexified using the second-order cone relaxation from [26]: $\pi_{a_h,t} - \pi_{a_t,t} \ge W_a \phi_{a,t}^2$. This relaxation is very tight [26].

When the gas system is not congested, the price of natural gas is relatively stable. However, during congestion and when some loads are being shed, natural gas prices increase sharply. The cost of gas in the objective function captures this behavior: For a junction j, it is specified with an almost-linear piecewise linear function for production and a high penalty $\cos\kappa_j$ for gas shedding. To be specific, let \mathcal{S}_j be a set of non-overlapping intervals covering $[0,\overline{s}_j^g]$, each with a distinct slope $c_{j,s}$ satisfying $c_{j,s} \leq c_{j,s+1}$ for all consecutive intervals $s,s+1\in\mathcal{S}_j$. Define an auxiliary nonnegative variable $s_{s,t}^g$ that represents the amount of gas supply from $s\in\mathcal{S}_j$ at time t. The objective function is then stated as Equation (2a). The model also includes constraint (2k) to link the gas variable at junction j with the auxiliary variables.

C. Physical and Economic Couplings

GFPPs are the physical and economic interface between the electrical power and gas networks. This section first describes the resulting coupling constraints before describing how the natural gas zonal prices are computed. Tables V and VI describe the parameters for the coupling.

TABLE VI VARIABLES FOR THE ELECTRICITY AND GAS COUPLING

$w_{b,t}$	1 if $b \in \mathcal{B}_u$ of $u \in \mathcal{U}$ is selected during $t \in \mathcal{T}$, 0 otherwise
$\rho_{u,t}$	Price of marginally selected bid of $u \in \mathcal{U}^g$ during $t \in \mathcal{T}$
$\psi_{k,t}$	Zonal price of natural gas in $k \in \mathcal{K}$ during $t \in \mathcal{T}$

The physical couplings between \mathcal{G}^e and \mathcal{G}^g can be formulated as follows $(t \in [T], j \in \mathcal{N} \cap \mathcal{V})$:

$$\gamma_{j,t} = \sum_{u \in \mathcal{U}(j) \cap \mathcal{U}^g} H_{u,2} p_{u,t}^2 + H_{u,1} p_{u,t} + H_{u,0}.$$
 (3)

The real power generation p of a GFPP induces a demand γ in the natural gas system. Equation (3) specifies the relationship between the real power generation of a GFPP and the amount of natural gas needed for the generation. In the equation, this relationship is approximated by a quadratic heat-rate curve, whose coefficients are given as H_u . The equation can be convexified like the Weymouth equation.

Since the level of power generation of the GFPPs determines the load in the gas system, the physical coupling also affects the natural gas prices. The price formation of natural gas, in turn, governs the profitability of GFPPs, which submit bids before the realization of gas prices. To capture these economic realities, the model introduces binary variables of the form $w_{b,t} \in \{0,1\}$ for each bid b of a GFPP to Problem (1): Variable $w_{b,t}$ indicates whether bid b is selected during time period b. Equation (1m) is then replaced by the following constraints (for all b is b in b in

$$\rho_{u,t} = \sum_{b \in [B_u - 1]} \beta_b(w_{b,t} - w_{b+1,t}) + \beta_{B_u} w_{B_u,t}, \forall u \in \mathcal{U}^g,$$
(4a)

$$0 \le s_{b,t}^e \le \overline{s}_b, \forall b \in \mathcal{B}_u, \ u \in \mathcal{U} \setminus \mathcal{U}^g, \tag{4b}$$

$$0 \le s_{b,t}^e \le \overline{s}_b w_{b,t}, \forall b \in \mathcal{B}_u, \ u \in \mathcal{U}^g, \tag{4c}$$

$$w_{b,t} \le o_{u,t}, \forall b \in \mathcal{B}_u, \ u \in \mathcal{U}^g,$$
 (4d)

$$\overline{s}_b w_{b+1,t} \le s_{b,t}, \forall b \in [1, B_u - 1]_{\mathbb{Z}}, \ u \in \mathcal{U}^g. \tag{4e}$$

Equations (4b) and (4c) are bound constraints for the bids submitted by the non-GFPPs and GFPPs respectively. Equation (4c) ensures that the indicator variable $w_{b,t}$ is one whenever bid b is used for time period t (i.e., $s_{b,t}^e>0$). Equation (4d) states that the bid of a generator can be selected only when it is committed and Equation (4e) ensures that the (b+1)th bid is selected only if the bid b is fully used. Accordingly, Equation (4a) states that $\rho_{u,t}$ is the maximum/marginal bid price of GFPP $u \in \mathcal{U}^g$ among its currently selected bids.

The economic coupling between the electricity and gas networks is enforced by *bid-validity constraints* that ensure that the marginal costs of producing electricity by GFPPs are lower than their marginal bid prices. Although the natural gas system is operated in a decentralized manner, the zonal price of natural gas ψ can be modeled as a function g of the market supply and demand, i.e., as a function of the binary and continuous variables of Problems (1) and (2), which are denoted by z and x. Under this assumption, the bid validity constraints can be expressed as

follows (for all $t \in [T]$):

$$\psi = g(z, x),\tag{5a}$$

$$\alpha_u \rho_{u,t} \ge [2p_{u,t}H_{u,2} + H_{u,1}] \psi_{k,t} o_{u,t},$$

$$\forall k \in \mathcal{K}, i \in \mathcal{V}(k), u \in \mathcal{U}(i) \cap \mathcal{U}^g,$$
 (5b)

where

$$2p_{u,t}H_{u,2} + H_{u,1}$$

is the derivative of the heat rate curve (i.e., Equation (3)) that represents the amount of natural gas needed for generating one additional unit of real power by GFPP u. The nonlinear term in the right-hand side of Equation (5b) is linearized by employing an exact McCormick relaxation. Accordingly, when a GFPP u is online, the right-hand side of Equation (5b) represents the realized natural gas price for generating one additional unit of real power by the GFPP u. Hence, Equation (5b) captures the fact that, when the realized natural gas price for generating one additional unit of real power by GFPP u is greater than its marginal bid price $\rho_{u,t}$, GFPP u is not profitable. This situation arises because GFPP u submits its bids before the realization of ψ . The bid validity constraint is expressed in Equation (5b) and ensures that only profitable GFPPs are committed. Note that, as discussed at length subsequently, α_u is best viewed as a part of the bid for GFPP u that reflects its risk aversion level; The larger α_u is (possibly greater than 100%), the less likely GFPP u is of being de-committed due to the bid validity constraint and the larger the risk u is willing to take in terms of natural gas prices. The bid validity constraints use the realized zonal gas prices from Equation (5a) and the maximum natural gas price (e.g., \$200 per mmBtu) multiplied by $[2\overline{p}_u H_{u,2} + H_{u,1}]$ as the upper bound of the continuous term in its right-hand side for the McCormick relaxation.

It remains to specify how to compute the zonal gas prices, i.e., the function g in Equation (5a). The UCGNA assumes that the nodal natural gas price at each junction j is given by the marginal cost of supplying natural gas at j. This marginal cost is the dual solution associated with the corresponding flux conservation constraint in Problem (2). The zonal natural gas prices ψ are then computed by averaging the nodal natural gas prices of a subset of junctions in the zone. Therefore, the zonal natural gas price ψ are given by linear functions of the dual solution to Problem (2).

Note that, by construction, the natural gas zonal prices ψ under normal operating conditions are given by the almost linear part of objective (2a). However, when the gas network is congested and load needs to be shed, the zonal prices increase sharply due to the high penalty $\cos \kappa_j$. As a result, the resulting model closely captures the behavior of the market during the 2014 polar vortex. Note also that the model does not shed the demand of the GFPPs. The model assumes that GFPPs buy natural gas at any cost to meet its commitment obligation. Once again, this captures the 2014 Polar Vortex situation where GFPPs were encouraged to buy the natural gas from the spot market at any cost for the sake of the power system reliability [3].

III. REFORMULATION OF THE UCGNA

This section shows how the UCGNA can be expressed as a MISOCP. Let variable subscripts e and g respectively denote the electricity and the gas systems. Let z_e and x_e respectively denote the vector of binary and continuous variables of the power system (i.e., Problem (1)) and let x_g be the vector of continuous variables of the gas system (i.e., Problem (2)). The UCGNA can be stated as a trilevel program²:

$$\min_{\substack{\boldsymbol{x}_e \ge 0, \boldsymbol{y}_g \\ \boldsymbol{z}_e \in \{0,1\}^m}} c_e^T \boldsymbol{x}_e + h^T \boldsymbol{z}_e$$
 (6a)

s.t.
$$z_e \in \mathcal{Z}$$
, (6b)

$$(\boldsymbol{x}_e, \boldsymbol{y}_g) = \underset{\boldsymbol{x}_e \ge 0, \boldsymbol{y}_g}{\operatorname{argmin}} c_e^T \boldsymbol{x}_e$$
 (6c)

s.t.
$$Ax_e + Bz_e \ge b$$
, (6d)

$$y_q \in \text{Dual sol. of } (7), \quad (6e)$$

$$E\boldsymbol{y}_{q} + M\boldsymbol{z}_{e} \ge h \tag{6f}$$

where \mathcal{Z} denotes the feasible region of the unit commitment problem (i.e., Equations (1b)-(1h)), the third level problem is defined as

$$\min_{\boldsymbol{x}_g \in \mathcal{K}} c_g^T \boldsymbol{x}_g : D_e \boldsymbol{x}_e + D_g \boldsymbol{x}_g \ge d, \tag{7}$$

and K is the proper cone denoting the domain of x_q .

The first-level problem (i.e., Equations (6a) and (6b)) formulates the unit-commitment problem (i.e., Equations (1a)–(1h) and Equation (4)). The unit-commitment decisions z_e from the first-level problem are then plugged into the second-level problem (i.e., Equation (6c)-(6d)), which formulates the economic dispatch problem (i.e., Equations (1j)–(1u)) and decides the hourly operating schedule of committed generating units. The economic dispatch decisions x_e determine natural gas demand of committed GFPPs and are plugged into the third-level problem (i.e., Problem (6e)), which formulates the natural gas problem (i.e., Problem (2) and Equation (3)). Then, the third level problem determines the resulting nodal prices for natural gas based on the dual solution y_g of the gas flux conservation constraints (i.e., Equation (2b)).

Equations (6a)–(6e) capture the current operating practice of the power system. Without Equation (6f), the first level captures the commitment decisions that are taken without consideration of the gas network. The second and third levels implement a Stackelberg game, where the dispatch decisions of the electricity system are followed by those of the natural gas network. *The novelty in the UCGNA is the bid-validity constraint (6f), which corresponds to Equation (5b)*: It ensures that only profitable GFPPs are selected in the first level and uses the dual variables of the third-level problem to do so, allowing the unit-commitment problem to anticipate the zonal prices of natural gas.

²From a game theoretic perspective, the problem at hand is a two-level problem (See Appendix A). However, for ease of deriving a single-level formulation in Theorem 1 and to make the UCGNA formulations more intuitive, the problem is posed as a tri-level.

The following theorem, whose proof is in Appendix B, shows that the tri-level problem can be reformulated as a single-level mathematical program. The proof uses strong duality on the third-level problem and lexicographic optimization to merge the second and third levels.

Theorem 1: Problem (6) can be asymptotically approximated by the following mathematical program:

$$\min \delta h^T \boldsymbol{z}_e + \delta c_e^T \boldsymbol{x}_e + (1 - \delta) c_a^T \boldsymbol{x}_a \tag{8a}$$

s.t.
$$z_e \in \mathcal{Z}, z_e \in \{0,1\}^m$$
, (8b)

$$Ax_e + Bz_e > b, \tag{8c}$$

$$D_e \mathbf{x}_e + D_a \mathbf{x}_a > d, \tag{8d}$$

$$\boldsymbol{y}_{e}^{T}(b - B\boldsymbol{z}_{e}) + \boldsymbol{y}_{q}^{T}d \ge \delta c_{e}^{T}\boldsymbol{x}_{e} + (1 - \delta)c_{q}^{T}\boldsymbol{x}_{g},$$
 (8e)

$$\boldsymbol{y}_{a}^{T} D_{a} \preceq_{\mathcal{K}^{*}} (1 - \delta) \boldsymbol{c}_{a}^{T}, \tag{8f}$$

$$\boldsymbol{y}_{e}^{T} \boldsymbol{A} + \boldsymbol{y}_{a}^{T} \boldsymbol{D}_{e} \le \delta \boldsymbol{c}_{e}^{T}, \tag{8g}$$

$$\frac{1}{1-\delta}E\boldsymbol{y}_g + M\boldsymbol{z}_e \ge h,\tag{8h}$$

$$x_e \ge 0, x_q \in \mathcal{K},$$
 (8i)

$$\boldsymbol{y}_e \ge 0, \boldsymbol{y}_g \ge 0, \tag{8j}$$

for some $\delta \in (0,1)$. Moreover, when $\delta \to 1$, the optimal solution of Problem (8) converges to the optimal solution of Problem (6).

Observe that Problem (8) has a bilinear term of $\mathbf{y}_e^T B \mathbf{z}_e$ in Equation (8e). Assuming that \mathbf{y} has an upper bound of $\overline{\mathbf{y}}$, this term can be rewritten using an exact McCormick relaxation to produce a MISOCP.

Remark 1: Problem (8) is best viewed as a "standard" MIS-OCP to which a constraint on the dual variables of its inner-continuous problem has been added. The "standard" MISOCP optimizes the joint electricity and natural gas problem

$$\min \delta h^T \boldsymbol{z}_e + \delta \boldsymbol{c}_e^T \boldsymbol{x}_e + (1 - \delta) \boldsymbol{c}_a^T \boldsymbol{x}_a \tag{9a}$$

s.t.
$$z_e \in \mathcal{Z}$$
, (9b)

$$Ax_e + Bz_e > b, (9c)$$

$$D_e \mathbf{x}_e + D_a \mathbf{x}_a \ge d, \tag{9d}$$

$$x_e > 0, x_g \in \mathcal{K}, z_e \in \{0, 1\}^m,$$
 (9e)

and the additional constraints

$$\frac{1}{1-\delta}Ey_g + Mz_e \ge h.$$

on the dual variables (y_e, y_g) of its inner continuous problem capture the bid validity. That is because Problem (8) consists of the following four main components: (i) primal constraints (e.g., Equations (8c), (8d), and (8i)) and (ii) dual constraints (e.g., Equations (8f), (8g), and (8j)) of the inner-continuous problem of Problem (9), (iii) the optimality condition (e.g., Equation (8e)) that states that the inner-continuous problem and its dual counterpart have the same objective value (note that the other direction holds by weak duality), and (iv) the bid validity constraints (e.g., Equation (8h)).

IV. SOLUTION APPROACH

This section briefly sketches how the MISOCP is solved. Problem (8) can be reformulated as

$$\min_{\boldsymbol{z}_e \in \mathbb{B}^n} \delta h^T \boldsymbol{z}_e + f(\boldsymbol{z}_e) \tag{10a}$$

s.t.
$$z_e \in \mathcal{Z}$$
. (10b)

where

$$f(\boldsymbol{z}_e) = \min \ \delta c_e^T \boldsymbol{x}_e + (1 - \delta) c_g^T \boldsymbol{x}_g$$
 (11a)

s.t.
$$A\boldsymbol{x}_e + B\boldsymbol{z}_e \ge b$$
, (11b)

$$D_e x_e + D_q x_q \ge d, (11c)$$

$$\boldsymbol{y}_{e}^{T}(b-B\boldsymbol{z}_{e}) + \boldsymbol{y}_{g}^{T}d \ge \delta c_{e}^{T}\boldsymbol{x}_{e} + (1-\delta)c_{g}^{T}\boldsymbol{x}_{g},$$
(11d)

$$\boldsymbol{y}_q^T D_q \preceq_{\mathcal{K}^*} (1 - \delta) c_q^T, \tag{11e}$$

$$\boldsymbol{y}_e^T \boldsymbol{A} + \boldsymbol{y}_q^T \boldsymbol{D}_e \le \delta \boldsymbol{c}_e^T, \tag{11f}$$

$$\frac{1}{1-\delta}E\boldsymbol{y}_g + M\boldsymbol{z}_e \ge h,\tag{11g}$$

$$\boldsymbol{x}_e \ge 0, \boldsymbol{x}_q \in \mathcal{K}, \boldsymbol{y}_e \ge 0, \boldsymbol{y}_q \ge 0.$$
 (11h)

The implementation applies a Benders decomposition on this formulation to solve Problem (8). Moreover, the dual of Problem (11) has a special structure that can be exploited by the dedicated Benders decomposition from [23]. The idea is to decompose the dual of Problem (11) into two more tractable problems. The extreme points and rays of these subproblems can be used to find the (feasibility and optimality) Benders cuts of Problem (11). The solution method also uses the acceleration schemes from [27], [28] which normalize the rays \hat{y} and perturb \hat{z}_e . The solution method also obtains feasible solutions periodically (e.g., every 30 iterations) heuristically by turning off violated generators. Finally, the solution method applies a preprocessing step to eliminate some invalid bids. It exploits the fact that the natural gas prices without the GFPP load gives a lower bound on the natural gas zonal prices. Therefore, the implementation solves Problem (2) with no GFPPs, i.e., $\gamma_{i,t} = 0$ for all $j \in \mathcal{V}, t \in [1, T]_{\mathbb{Z}}$. Those bids violating the bid-validity constraint with regard to these zonal prices are not considered further.

V. DESCRIPTION OF THE DATA SETS

The UCGNA model is evaluated on the gas-grid test system from [1], which is representative of the natural gas and electric power systems in the Northeastern United States. This test system is composed of the IEEE 36-bus NPCC electric power system [29] and a multi-company gas transmission network covering the Pennsylvania-To-Northeast New England area in the United States [1]. The data for the test system can be found online at https://github.com/lanl-ansi/GasGridModels.jl and we only decrease nodal pressure bounds by a factor of 3 to get an interesting test case.

The test system consists of 91 generators of various types (e.g., hydro, gas-fueled, coal-fired, etc.). The unit-commitment

data for these generators (e.g., generator offer curves including start-up and no-load costs and operational parameters such as minimum run time) was obtained from the RTO unit commitment test system [30]. Each generator in the gas-grid test system is assigned the unit commitment data adapted to its fuel-type and megawatt capacity. To introduce more variety on bidding behaviors, we modify some offer curves.

The data sets account for the fact that prices in the gas spot market in the United States is zonal [31], and the gas-grid test case consists of two natural gas pricing zones: Transco Zone 6 non NY and Transco Leidy Line. The Transco Leidy Line represents the natural gas prices in the Marcellus Shale production area, which has a wealth of natural gas. On the other hand, the Transco Zone 6 non NY represents the natural gas prices near consumption points. Therefore, a large difference in prices between these two pricing zones implies a scarcity of transmission capacities between these two points. During normal operations, the average natural gas prices in the Transco Zone 6 non NY and the Leidy Line are around \$3/mmBtu and \$1.5/mmBtu respectively. The slopes $c_{j,s}$ at junction $j \in \mathcal{V}$ (see Section (II-B)) are chosen to be around these numbers. The penality cost for load shedding κ_i is set as \$130/mmBtu for all junctions. The results are given for a single time-period (i.e., T = 1).

VI. CASE STUDY

This section analyzes, under various operating conditions, the behavior of the UCGNA on the realistic test system described in Section V. The results are compared with current practices. The case study varies the level of stress on both the electrical power and gas systems. For the electrical power system, the load is uniformly increased by 30% and 60%. For the gas system, the load is uniformly increased by 10% up to 130%. Parameters η_e and η_g respectively represent the stress level imposed on the electrical power and gas systems. In the results, (A) denotes existing practices and (B) the UCGNA model. Solutions for (B) are obtained with a wall-clock time limit of 1 hour, while solutions for (A) is obtained by the following procedure:

- i) Solve the power model (i.e., Problem (1));
- ii) Retrieve the demand of GFPPs using Equation (3) and plug it into the gas model (i.e., Problem (2));
- Solve the gas model and compute the natural gas zonal prices using the dual values associated with the flux conservation constraints;
- iv) Based on the zonal prices, determine the set of GFPPs violating the bid-validity constraint (i.e., Equation (5b)) and compute the loss of such GFPPs by multiplying the violation, i.e., the difference between the marginal gas price and the marginal bid price, with the scheduled amount of power generation.

The behaviors of (A) and (B) in the normal, stressed, and highly-stressed power systems are compared in Figs. 1, 2, and 3 respectively. In each figure, (a) and (c) display the system costs and natural gas prices of (A), and (b) and (d) display those of (B). More precisely, (a) and (b) present the total cost breakdown in terms of the cost of electrical power system, the cost of the

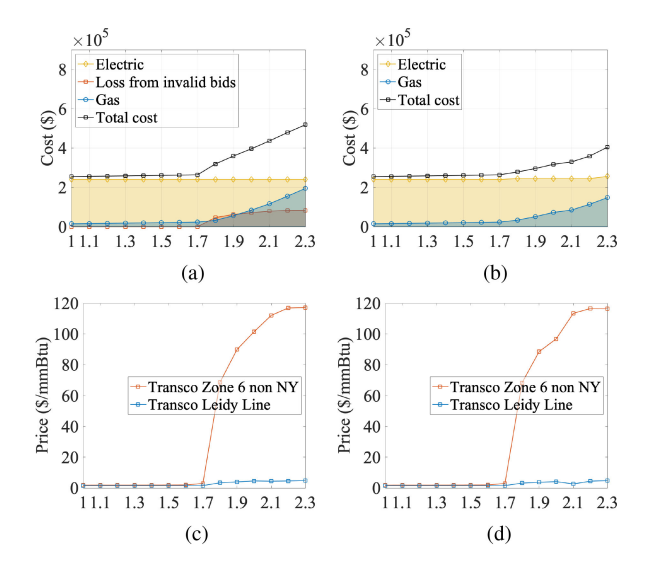


Fig. 1. Results for the normal operating conditions of the electrical power system ($\eta_e = 1$), where x-axis represents η_g . (a) System costs (A). (b) System costs (B). (c) Natural gas prices (A). (d) Natural gas prices (B).

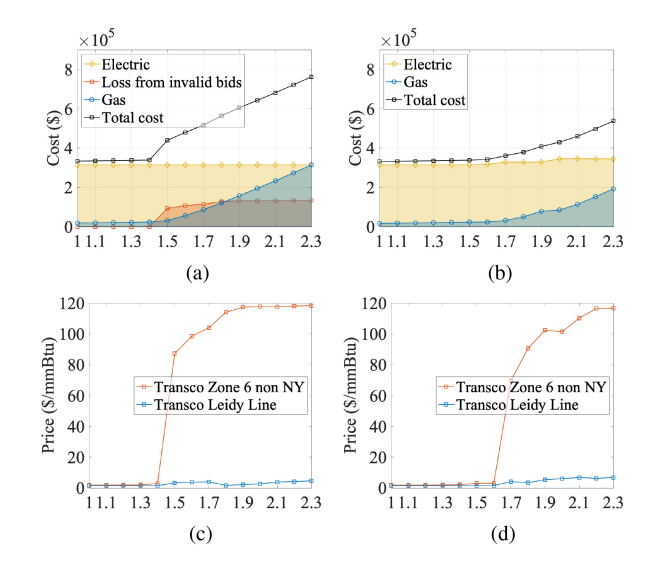


Fig. 2. Results for the stressed electrical power system ($\eta_e=1.3$), where x-axis represents η_g . (a) System costs (A). (b) System costs (B). (c) Natural gas prices (A). (d) Natural gas prices (B).

gas system, and the economic loss from invalid bids. (c) and (d) depict the natural gas zonal prices in each pricing zone.³

Figs. 1(a) and 1(c) show that the gas system cost gradually increases as η_g increases up to 1.7, then it grows rapidly from $\eta_g=1.8$ on. The rapid increase is due to load shedding (see Section II-B) and leads to natural gas price spikes in Transco Zone 6 non NY. The large difference between the prices in Zone 6 and Leidy Line indicates that the load shedding occurs due to the lack of transmission capacity between these two points, not because of a lack of gas supply. Due to the gas price spike in Transco Zone 6 non NY, some bids of GFPPs become invalid and incur some losses, which increases the total cost. On the

³Note that, as η_g increases, the total cost of (A) always increases, while the cost of (B) temporarily decreases sometimes. This is due to the presense of optimality gaps for some hard instances.

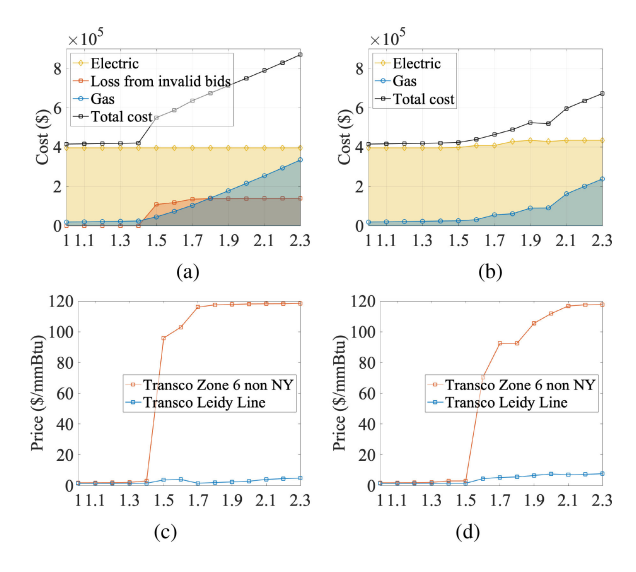


Fig. 3. Results for the highly-stressed electrical power system ($\eta_e = 1.6$), where x-axis represents η_g . (a) System costs (A). (b) System costs (B). (c) Natural gas prices (A). (d) Natural gas prices (B).

other hand, for (B), the electrical power system cost is slightly higher than for (A), but it does not incur any economic loss from invalid bids and the overall cost is lower. Observe also that model (A) captures the same behavior as in the 2014 polar vortex. Additionally, observe that the gas price in the Zone 6 region is also exhibiting sharp increases in model (B). However, this peak has significantly less impact for (B) given the different commitment decisions.

The differences in behavior between systems (A) and (B) become clearer as the load increases in the electrical power system. For the stressed power system, displayed in Fig. 2, the difference between the total cost of (A) and (B) becomes very large: There are many invalid bids for (A), which puts the reliability of the power system at high risk and induces an electricity price peak. The price of gas and the economic losses both increase significantly in (A) and the increases start at stress level 1.5 for the gas network. In contrast, (B) maintains a reliable operation independently of the stress imposed on the natural gas system. The price of gas increases obviously but less than in (A) and the cost of the power system remains stable. The peak in gas price only starts at stress level 1.7, showing that (B) delays the impact of congestion in the gas networks by making better commitment decisions.

Fig. 3 shows the benefits of (B) over (A) become even more substantial when both systems are highly stressed. Observe that the cost of the electrical power system remains stable once again in (B) and that the cost of the gas network increases reasonably. In contrast, Model (A) exhibits significant increases in gas prices and economic cost from invalid bids. These results indicate that bringing gas awareness in unit commitment brings significant benefits in congested networks. By choosing commitment decisions that ensure bid validity, the UCGNA brings substantial cost and reliability benefits for congested situations like the 2014 polar vortex.

The great cost and reliability benefits of (B) are owing to better commitment decisions that anticipate the future state of the gas system. Table VII in Appendix C summarizes some statistics on committed generators under the highly stressed power system. As the gas load increases, some of the GFPPs in (T) are no longer committed and the lost generation is replaced by generators of different types or GFPPs with reasonable bid prices. More specifically, Fig. 4 in Appendix C shows the commitment decision of (A) and (B) for $(\eta_e, \eta_g) = (1.6, 2.3)$. The numbers in black in Figs. 4(a) and 4(c) report the number of committed GFPPs on the corresponding bus; Those in Figs. 4(b) and 4(d) display the number of committed non-GFPPs. In Figs. 4(a), the numbers in red on the bottom right corner of some buses represent the number of committed GFPPs located at the bus without bid validity. Most invalid GFPPs in Fig. 4(a) are turned off in Fig. 4(c) and replaced by some non-GFPPs as Fig. 4(d) indicates.

Finally, Table VIII in Appendix C summarizes the objective value and the optimality gap of (B) for each instance. For 16 out of 42 instances, the algorithm times out (wall-clock limit time of 1 hour) and it reports sub-optimal solutions whose optimality gaps are presented in columns denoted by (ii).

Suboptimal solutions are not desirable in market clearing, so future research should be devoted to improve these computational results further. Note however that these suboptimal results arise for highly congested situations in both networks. In such circumstances, operators are typically switching to an emergency reliability state, as was the case during the polar vortex events [3]. The results thus demonstrate that the UCGNA bring significant benefits for reliability of gas-grid networks.

VII. DISCUSSION

The contribution of this paper is best viewed as two synergistic component: (1) a richer bid language for GFPPs allowing to express their risk aversion and (2) a market clearing mechanism, that use the more expressive bids to obtain the UCGNA, a gas-aware unit commitment for the electricity market. This section discusses the practical applicability and implication of the UCGNA as an alternative market clearing mechanism to the current practice.

A potential criticism of the UCGNA is the assumption that the power system operator has partial (or full) knowledge on the gas demand forecast and the gas network, which may require some level of cooperation of the natural gas system. It should be noted that both the electricity and natural gas markets have been wishing for measures that address the risks stemming from inter-dependencies between the two networks. Continuous development of regulations on these two systems reflects the market needs; For example, FERC Order 787 permits electricity and natural gas transmission operators to share, with each other, information that they deem necessary to promote the reliability and integrity of their systems [32]. When the natural gas demand forecast and the gas network data are shared, the UCGNA has the potential to enhance the reliability and efficiency of both systems, as demonstrated by the detailed case study in Section VI. Indeed, the results show that, in congested environments, the gas-aware unit commitment reduces the gas system cost and postpones the natural gas price spikes. This benefit would incentivize gas transmission operators to cooperate. Even without the cooperation of the natural gas system, the proposed model can still be used with natural gas demand forecast that is obtained by the power system operator, as well as an incomplete description of the natural gas networks. The quality of the estimate, however, would improve as the power system operator acquire more accurate information about the gas system.

It is important to note that the UCGNA enables the GFPPs to hedge against risks induced by volatile natural gas prices. The main purpose of day-ahead markets is to produce a dispatch that anticipates and hedges against uncertainty that are observed in real time [33], [34]. In addition, the market should provide instruments that allow their participants to hedge risks so that a competitive equilibrium corresponds to the social optimum [35]. The current practice, however, neither anticipates uncertainty in the natural gas system nor has a market instrument for the GF-PPs to hedge against their volatile operating costs. The GFPPs currently lack the ability to reflect changes to their operating costs after the reoffer period [3] and they have restrictive bidding language that cannot correctly incorporate their risk-appetite. Hence, the GFPPs may endure severe consequences when incorrectly forecasting natural gas prices. This makes the GFPPs less competitive and may eventually discourage them from staying in the market, which is highly undesirable, especially for power systems with a significant portion of renewable energy. The UCGNA, on the other hand, allows the GFPPs to make conditional bids: their bids are only valid as long as the realized natural gas prices are anticipated not to be much higher than their forecasts. It should be noted that, in the bid validity constraint, the system operator accepts different risk-aversion levels of each GFPP u through α_u .

This paper also advocates for a richer bidding languages so that GFPPs have more flexibility in the UCGNA. Indeed, ideally, a GFPP should be able to submit multiple bids, each of which is conditional on an anticipated range of realized natural gas prices and has an associated threshold α_u . This enables the commitment decision to correctly reflect the "actual" price that the GFPP is willing to offer, which is conditional on natural gas prices. This can be naturally incorporated into the UCGNA by introducing additional binary variables in the first level that represent the expected price range of natural gas.

Another potential criticism of the UCGNA concerns the transparency of the natural gas price estimation that will be endogenously obtained and used in the UCGNA. One may question whether the GFPPs would be willing to accept the commitment decision when they are de-committed due to the bid validity constraints. In practice, the estimated natural gas prices in the UCGNA are largely dependent on natural gas demand forecast. The disclosure of natural gas demand forecast to GFPPs before the bid submission period closes thus gives GFPPs the opportunity to design their bidding strategy accurately.

Note also that the economic feedback from the natural gas system affects the commitment and dispatch decisions in a completely discrete manner: Once the binary decisions are committed and ensure that the bid validity constraints are met, the second level clears the market in the same way as in the

current practice. Thus, the current market properties (e.g., revenue adequacy of ISOs and cost recovery for committed generators achieved under some assumptions/market instruments) also applies to the UCGNA. Recently, several papers proposed stochastic energy-only market clearing mechanisms to address undesirable properties of the current market introduced by the increasing penetration of intermittent generators [33], [34], [36], [37]. The UCGNA can be adapted to embody a single-settlement stochastic dispatch (e.g., [34]) in the second level problem, which would result in a stochastic economic feedback from the gas system. In this case, the bid validity constraint should be formulated differently to accommodate the uncertainty (e.g., by using chance constraints). Future research will be devoted to incorporating a stochastic dispatch into the UCGNA.

VIII. CONCLUSION

The 2014 polar vortex showed how interdependencies between the electrical power and gas networks may induce significant economic and/or reliability risks under heavy congestion. This paper has demonstrated that these risks can be effectively mitigated by making unit commitment decisions informed by the physical and economic couplings of the gas-grid network. The resulting Unit Commitment with Gas Network Awareness (UCGNA) model builds upon the standard unit commitment used in current practices but also reasons about the feasibility of gas transmission feasibility and the profitability of committed GFPPs. In particular, the UCGNA introduces bid-validity constraints that ensure the economic viability of committed GFPPs, whose marginal bid prices must be higher than the marginal natural gas prices by some percentage α_u . Section VII also advocated for a richer bidding language that the GFPPs can use to express more complex bids capturing different levels of natural gas prices.

The UCGNA is a three-level model whose bid validity constraints operate on the dual variables of flux conservation constraints in the gas network, which calculate the marginal cost of gas for producing a unit of electricity. It can be formulated as a Mixed-Integer Second-Order Cone Program (MISOCP) and solved using a dedicated Benders decomposition approach. The case study, based on a modeling of the gas-grid network in the North-East of the United States, shows that the UCGNA has significant benefits compared to the existing operations: It is capable to ensure valid bids even at highly-stressed levels, while only increasing the cost of gas and electricity in a reasonable way. In contrast, the existing operating practices induce significant economic losses and gas price increases.

In summary, the UCGNA allows GFPPs to hedge against their volatile operating costs by providing bids that are conditional to anticipated natural gas prices. The resulting bids effectively give them an opportunity to "withdraw" their bids when the gas prices are too high. The UCGNA also helps system operators to avoid the default of GFPPs and fuel supply issues that have plagued the gas network during the polar vertex events. The current market properties are maintained since the economic feedback only affects the first level solution. Future research will be devoted to adapting the second-level problem to a stochastic

dispatch problem and further improving the solution techniques to solve the UCGNA, including the use of cut bundling and Pareto-optimal cuts.

APPENDIX A

EQUIVALENCE OF PROBLEM (6) TO A TWO-LEVEL PROBLEM

Consider the following two-level problem:

$$\min_{\substack{\boldsymbol{x}_e \ge 0, \boldsymbol{y}_g \\ \boldsymbol{z}_e \in \{0,1\}^m}} c_e^T \boldsymbol{x}_e + h^T \boldsymbol{z}_e \tag{12a}$$

s.t.
$$z_e \in \mathcal{Z}$$
, (12b)

$$Ax_e + Bz_e \ge b, (12c)$$

$$\boldsymbol{y}_g \in \text{Dual sol. of } \min_{\boldsymbol{x}_g \in \mathcal{K}} c_g^T \boldsymbol{x}_g$$
 (12d)

s.t.
$$D_e x_e + D_q x_q \ge d$$
, (12e)

$$E\boldsymbol{y}_{a} + M\boldsymbol{z}_{e} \ge h, \tag{12f}$$

where the first level (i.e. Equations (12a), (12b), and (12c)) represents the power system's action taken by UC/ED problem, and the second level problem represents the response of the natural gas system (i.e., natural gas price y_g). In addition, the bid validity constraint (i.e., Constraint (12f)) affects the power system's commitment decisions based on the response of the gas system. Hence the power system can be viewed as a "leader" and the gas system as a "follower" in the Stackelberg game.

Let $(\hat{\boldsymbol{z}}_e, \hat{\boldsymbol{x}}_e, \hat{\boldsymbol{y}}_g)$ be a feasible solution of Problem (6). Then, it is easy to see that $(\hat{\boldsymbol{z}}_e, \hat{\boldsymbol{x}}_e, \hat{\boldsymbol{y}}_g)$ is also a feasible solution to Problem (12) with the same objective function value.

Conversely, consider a feasible solution to Problem (12), $(\tilde{\boldsymbol{z}}_e, \tilde{\boldsymbol{x}}_e, \tilde{\boldsymbol{y}}_g)$. Note that, with \boldsymbol{z}_e fixed to $\tilde{\boldsymbol{z}}_e \in \mathcal{Z}$, $(\tilde{\boldsymbol{x}}_e, \tilde{\boldsymbol{y}}_g)$ is also an optimal solution of the lower level problem of Problem (6). This is because the second level decision (i.e., \boldsymbol{x}_e) is not affected by the third level decision, thus $\boldsymbol{x}_e = \tilde{\boldsymbol{x}}_e$ is an optimal solution of the second level problem. Then, when \boldsymbol{x}_e fixed to $\tilde{\boldsymbol{x}}_e, \boldsymbol{y}_g = \tilde{\boldsymbol{y}}_g$ is a valid response of the gas system. Accordingly, Constraint (12f) is satisfied and hence $(\tilde{\boldsymbol{z}}_e, \tilde{\boldsymbol{x}}_e, \tilde{\boldsymbol{y}}_g)$ is feasible for Problem (6) with the same objective value. Therefore, the two problems are equivalent.

APPENDIX B PROOF OF THEOREM 1

Proof: By strong duality of the third-level optimization in Problem (6), the lower-level problem (i.e., second- and third-level) of Problem (6) is equivalent to:

$$(\boldsymbol{x}_e, \boldsymbol{y}_g) = \underset{\boldsymbol{x}_e \ge 0, \boldsymbol{y}_g}{\operatorname{argmin}} c_e^T \boldsymbol{x}_e$$
 (13a)

s.t.
$$Ax_e + Bz_e \ge b$$
, (13b)

$$egin{aligned} oldsymbol{y}_g &= \underset{oldsymbol{x}_g \in \mathcal{K}, oldsymbol{y}_g \geq 0}{\operatorname{s.t.}} & c_g^T oldsymbol{x}_g \ & ext{s.t.} & D_e oldsymbol{x}_e + D_g oldsymbol{x}_g \geq d, \ & oldsymbol{y}_a^T (d - D_e oldsymbol{x}_e) \geq c_a^T oldsymbol{x}_g, \end{aligned}$$

$$\mathbf{y}_{q}^{T}D_{q} \preceq_{\mathcal{K}^{*}} c_{q}.$$
 (13c)

where K^* denotes the dual cone of K. The first and third constraints of Problem (13c) state the primal and dual feasibility

of the third-level problem, while the second constraint ensures their optimality.

Equation (13b) (i.e., the constraint of the upper level problem of Problem (13)) does not involve the lower-level variables (i.e., x_g and y_g of Problem (13c)), which means the upper-level solution is not affected by the solutions to the lower-level problem. Problem (13) can thus be solved in two steps: (i) solve the upper-level problem and obtain \bar{x}_e , (ii) solve the lower-level problem with x_e fixed as \bar{x}_e and obtain \bar{y}_g . Accordingly, Problem (13) can be expressed as a Lexicographic optimization problem [38] as follows:

$$(\boldsymbol{x}_e, \boldsymbol{y}_g) = \underset{\boldsymbol{x}_e \ge 0, \boldsymbol{x}_g \in \mathcal{K}, \boldsymbol{y}_g \ge 0}{\operatorname{argmin}} < c_e^T \boldsymbol{x}_e, c_g^T \boldsymbol{x}_g >$$
 (14a)

s.t.
$$A\boldsymbol{x}_e + B\boldsymbol{z}_e \ge b,$$
 (14b)

$$D_e \mathbf{x}_e + D_a \mathbf{x}_a \ge d, \tag{14c}$$

$$\boldsymbol{y}_g^T(d - D_e \boldsymbol{x}_e) \ge c_g^T \boldsymbol{x}_g, \quad (14d)$$

$$\boldsymbol{y}_g^T D_g \preceq_{\mathcal{K}^*} c_g. \tag{14e}$$

The optimal solution $(\bar{x}_e, \bar{x}_g, \bar{y}_g)$ of Problem (14) satisfies the following conditions:

$$\bar{x}_e = \underset{\boldsymbol{x}_e \ge 0, \boldsymbol{x}_g \in \mathcal{K}}{\operatorname{argmin}} \quad c_e^T \boldsymbol{x}_e$$
 (15a)

s.t.
$$Ax_e \ge b - Bz_e$$
, (15b)

$$D_e \mathbf{x}_e + D_g \mathbf{x}_g \ge d. \tag{15c}$$

$$(\bar{x}_g, \bar{y}_g) = \underset{\boldsymbol{x}_g \in \mathcal{K}, \boldsymbol{y}_g \ge 0}{\operatorname{argmin}} \quad c_g^T \boldsymbol{x}_g \tag{16a}$$

s.t.
$$D_a \boldsymbol{x}_a \ge d - D_e \bar{\boldsymbol{x}}_e$$
, (16b)

$$\boldsymbol{y}_{q}^{T}(d - D_{e}\bar{x}_{e}) \ge c_{q}^{T}\boldsymbol{x}_{q},$$
 (16c)

$$\boldsymbol{y}_g^T D_g \preceq_{\mathcal{K}^*} c_g. \tag{16d}$$

Observe that any feasible (\hat{x}_g, \hat{y}_g) of Problem (16) is optimal. That is because, by strong duality forced in Equation (16c), (\hat{x}_g, \hat{y}_g) satisfies the following conditions:

$$\hat{x}_g = \underset{\boldsymbol{x}_g \in \mathcal{K}}{\operatorname{argmin}} \quad c_g^T \boldsymbol{x}_g \tag{17a}$$

s.t.
$$D_a \mathbf{x}_a \ge d - D_e \bar{\mathbf{x}}_e$$
. (17b)

$$\hat{y}_g = \underset{\boldsymbol{y}_g \ge 0}{\operatorname{argmax}} \quad \boldsymbol{y}_g^T (d - D_e \bar{x}_e)$$
 (18a)

s.t.
$$\boldsymbol{y}_{g}^{T} D_{g} \preceq_{\mathcal{K}^{*}} c_{g}$$
. (18b)

Accordingly, using the weighted-sum method [38] for Lexicographic optimization problems and the optimality conditions of Problem (14), given in Problems (15) and (17)–(18), we approximate Problem (14) as follows:

$$\min_{\boldsymbol{x}_e \ge 0, \boldsymbol{x}_g \in \mathcal{K}} \delta c_e^T \boldsymbol{x}_e + (1 - \delta) c_g^T \boldsymbol{x}_g$$
 (19a)

s.t.
$$Ax_e + Bz_e \ge b$$
, (19b)

$$D_e \mathbf{x}_e + D_a \mathbf{x}_a \ge d, \tag{19c}$$

for some $\delta \in (0,1)$, and \pmb{y}_g is obtained by the dual solution associated with Equation (19c).

As a result, Problem (6) can be approximated by

$$\min \quad \delta h^T \boldsymbol{z}_e + \delta \boldsymbol{c}_e^T \boldsymbol{x}_e + (1 - \delta) \boldsymbol{c}_q^T \boldsymbol{x}_q \tag{20a}$$

s.t.
$$z_e \in \mathcal{Z}$$
, (20b)

$$(\boldsymbol{x}_e, \boldsymbol{x}_g, \boldsymbol{y}_g) = \text{Primal \& dual opt. sol. of (19)}, (20c)$$

$$\frac{1}{1-\delta}E\boldsymbol{y}_g + M\boldsymbol{z}_e \ge h,,\tag{20d}$$

$$\boldsymbol{x}_e \ge 0, \boldsymbol{x}_q \in \mathcal{K}, \boldsymbol{y}_e \ge 0, \boldsymbol{y}_q \ge 0, \tag{20e}$$

$$\boldsymbol{z}_e \in \{0, 1\}^m. \tag{20f}$$

Hence, by strong duality of Problem (19), stated in Equation (8e), Problem (8) is equivalent to Problem (20).

It remains to show that Problem (8) is indeed an asymptotic approximation of Problem (6). Replacing y_e with y_e/δ and y_g with $y_g/(1-\delta)$ in Problem (8) gives the following equivalent problem:

$$\min \quad \delta h^T \boldsymbol{z}_e + \delta c_e^T \boldsymbol{x}_e + (1 - \delta) c_q^T \boldsymbol{x}_q \tag{21a}$$

s.t.
$$z_e \in \mathcal{Z}$$
, (21b)

$$Ax_e + Bz_e \ge b, (21c)$$

$$D_e \mathbf{x}_e + D_q \mathbf{x}_q \ge d, (21d)$$

$$\boldsymbol{y}_{e}^{T}(b-Bz_{e})-c_{e}^{T}\boldsymbol{x}_{e}\geq\frac{1-\delta}{\delta}\left[c_{g}^{T}\boldsymbol{x}_{g}-\boldsymbol{y}_{g}^{T}d\right],$$
(21e)

$$\boldsymbol{y}_q^T D_g \preceq_{\mathcal{K}^*} c_q^T, \tag{21f}$$

$$\boldsymbol{y}_{e}^{T}\boldsymbol{A} + \frac{1-\delta}{\delta}\boldsymbol{y}_{g}^{T}\boldsymbol{D}_{e} \leq \boldsymbol{c}_{e}^{T}, \tag{21g}$$

$$E\boldsymbol{y}_g + M\boldsymbol{z}_e \ge h, \tag{21h}$$

$$\boldsymbol{x}_e \ge 0, \boldsymbol{x}_g \in \mathcal{K}, \boldsymbol{y}_e \ge 0, \boldsymbol{y}_g \ge 0,$$
 (21i)

$$\boldsymbol{z}_e \in \{0, 1\}^m. \tag{21j}$$

Let $P(\hat{z}_e)$ and $\widehat{P}(\hat{z}_e)$ denote Problems (14) and (21) in which the binary variables z_e are fixed to some $\hat{z}_e \in \{0,1\}^m$. Let $(\hat{x}_e,\hat{x}_g,\hat{y}_e,\hat{y}_g)$ be the optimal solution of $\widehat{P}(\hat{z}_e)$. Note that, as $\delta \to 1$, Equations (21e) and (21g) become as follows:

$$\boldsymbol{y}_e^T(b - B\hat{\boldsymbol{z}}_e) \ge c_e^T \boldsymbol{x}_e, \tag{22a}$$

$$\mathbf{y}_e^T A < c_e^T, \tag{22b}$$

which implies that \hat{x}_e and \hat{y}_e approximate the optimal primal and dual solutions of Problem (15) when z_e is fixed as \hat{z}_e . This is because \hat{x}_e is feasible for (15) (by Equation (21c)), $(\hat{y}_e, 0)$ becomes feasible to the dual of Problem (15) as δ approaches 1 (by Equation (22b)), and together they satisfy the strong duality condition of Equation (22a) as δ becomes closer to 1 (by Equation (22a)). Therefore, as $\delta \to 1$, (\hat{x}_e, \hat{y}_e) becomes a

feasible solutions of $P(\hat{z}_e)$ and has the same optimal objective value.

Moreover, combining Equations (21e) and (21g) gives

$$(\text{Equation } (21e)) - \hat{x}_e$$

$$\times (\text{Equation } (21g))$$

$$\rightarrow \hat{y}_e^T (b - B\hat{z}_e - A\hat{x}_e) + \frac{1 - \delta}{\delta}$$

$$\times \hat{y}_g^T (d - D_e \hat{x}_e) \ge \frac{1 - \delta}{\delta} c_g^T \hat{x}_g$$

$$\rightarrow \hat{y}_g^T (d - D_e \hat{x}_e) \ge c_g^T \hat{x}_g, \tag{23a}$$

where the last derivation follows from Equation (21c) and $y_g \ge 0$. Therefore, \hat{x}_g and \hat{y}_g are the optimal solutions of Problem (16) when x_e is fixed as \hat{x}_e (since its feasibility is guaranteed by Equations (21d) and (21f), while the optimality is guaranteed by Equation ((23a))).

In summary, \hat{x}_e is an approximate solution of $P(\hat{z}_e)$ that becomes increasingly close to the optimal solution of Problem $P(\hat{z}_e)$ as $\delta \to 1$, and \hat{y}_g is the exact response of the follower with respect to \hat{x}_e for any $\delta \in (0,1)$. Therefore, the approximation may sacrifice the leader's optimality when δ is not large enough, but it always gives a feasible solution.

APPENDIX C

TABLE VII

STATISTICS ON COMMITTED GENERATORS FOR THE STRESSED ELECTRICAL POWER SYSTEM ($\eta_e=1.6$): The First Seven Columns Display the Number of Committed Generators With Respect to Its Fuel Type, Where (O) Oil, (C) Coal, (G) Gas, (H) Hydro, (R) Refuse, (N) Nuclear, (E) Others, and the Last Two Columns Show the Number of Committed GFPPs in Each Pricing Zone, Where (T) Transco Zone 6 Non NY and (L) Transco Leidy Line

$\overline{\eta_g}$				(H)					
1.0	7	6	12	11	0	12	3	8	4
1.6	8	6	10	11	0	13	3	6	4
2.3	9			11			3	4	4

TABLE VIII
SOLUTION STATISTICS FOR (B), WHERE COLUMN (I) DENOTES THE FINAL
OBJECTIVE VALUE OF (B) FOR EACH INSTANCE AND COLUMN (II) REPRESENTS
THE OPTIMALITY GAP (TIME LIMIT: ONE HOUR)

η_e	1		1.3		1.6	
	(i)	(ii)	(i)	(ii)	(i)	(ii)
1	255301.0	0.0	332123.0	0.0	415315.0	0.0
1.1	256502.0	0.0	333333.0	0.0	416530.0	0.0
1.2	257706.0	0.0	334548.0	0.0	417759.0	0.0
1.3	258915.0	0.0	335776.0	0.0	419015.0	0.0
1.4	260132.0	0.0	337036.0	0.0	420548.0	0.0
. 1.5	261364.0	0.0	338564.0	0.0	423466.0	0.0
1.6	262613.0	0.0	342066.0	0.3	439254.0	2.1
1.7	264019.0	0.0	361089.0	3.5	463746.0	2.0
1.8	278679.0	1.8	379532.0	3.2	489011.0	6.2
1.9	296251.0	1.3	408407.0	3.3	524533.0	7.4
2	317619.0	0.0	430415.0	4.2	519026.0	3.7
2.1	329801.0	0.0	460127.0	4.3	596449.0	5.0
2.2	358828.0	0.0	497952.0	4.0	635128.0	5.0
2.3	405022.0	0.0	537874.0	0.0	672876.0	0.0

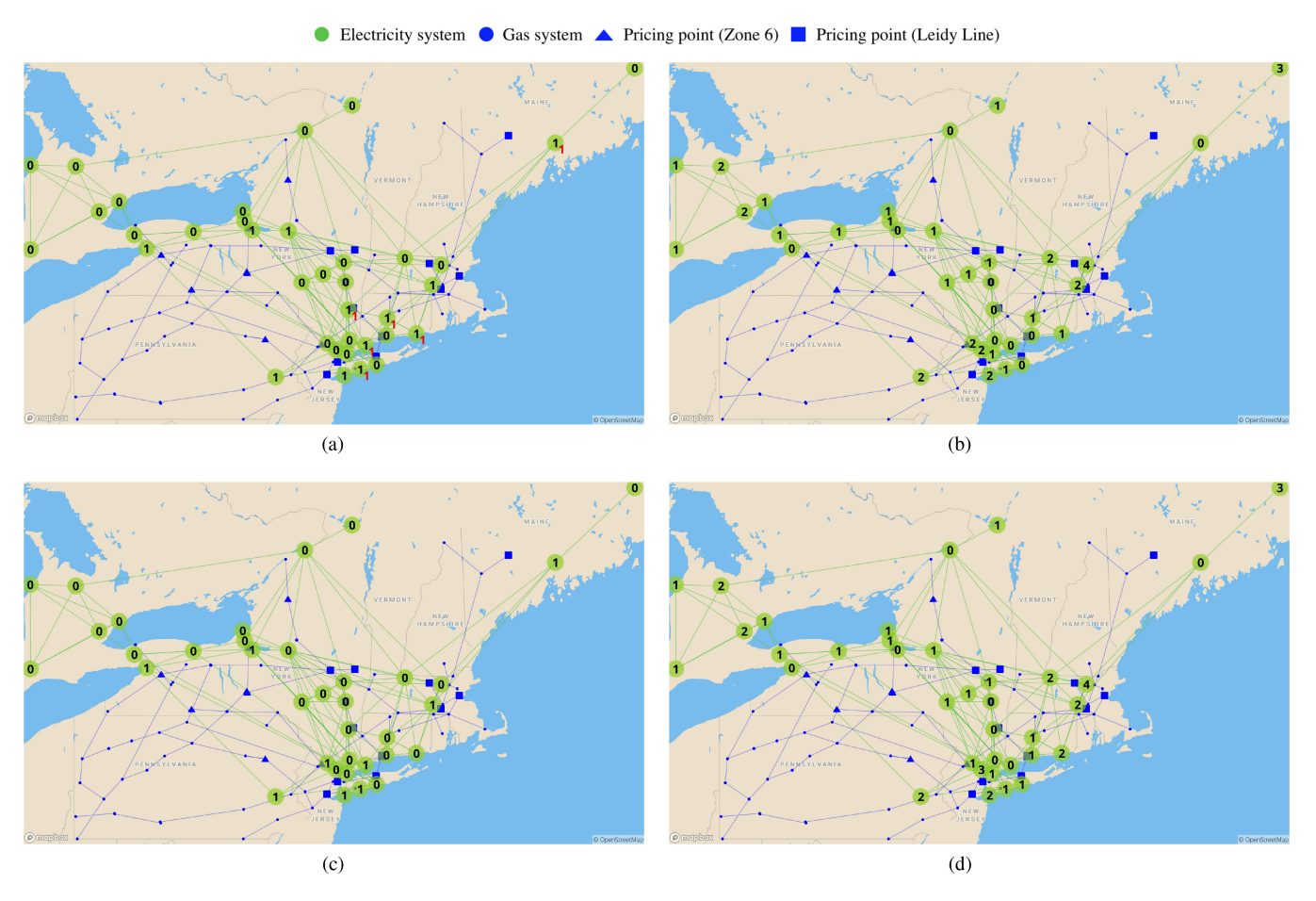


Fig. 4. Results for the highly-stressed condition $(\eta_e, \eta_g) = (1.6, 2.3)$. (a) Number of committed GFPPs (A). (b) Number of committed non-GFPPs (A). (c) Number of committed GFPPs (B).

ACKNOWLEDGMENT

The authors would like to thank the reviewers for their comments and suggestions that helped them clarify the paper, and also would like to thank M. Ferris for some insightful comments on this paper.

REFERENCES

- R. Bent, S. Blumsack, P. Van Hentenryck, C. Borraz-Sánchez, and M. Shahriari, "Joint electricity and natural gas transmission planning with endogenous market feedbacks," *IEEE Trans. Power Syst.*, vol. 33, no. 6, pp. 6397–6397, Nov. 2018.
- [2] "Analysis of operational events and market impacts during the January 2014 cold weather events," PJM, Norristown, PA, USA, 2014.
- [3] "Ruling in docket el14-45-000," FERC, Washington, DC, USA, 2015.
- [4] C. Liu, M. Shahidehpour, Y. Fu, and Z. Li, "Security-constrained unit commitment with natural gas transmission constraints," *IEEE Trans. Power Syst.*, vol. 24, no. 3, pp. 1523–1523, Aug. 2009.
- [5] C. Liu, M. Shahidehpour, and J. Wang, "Coordinated scheduling of electricity and natural gas infrastructures with a transient model for natural gas flow," *Chaos: Interdisciplinary J. Nonlinear Sci.*, vol. 21, no. 2, 2011, Art. no. 025102.
- [6] A. Martinez-Mares and C. R. Fuerte-Esquivel, "A unified gas and power flow analysis in natural gas and electricity coupled networks," *IEEE Trans. Power Syst.*, vol. 27, no. 4, pp. 2156–2166, Nov. 2012.
- [7] C. M. Correa-Posada and P. Sanchez-Martin, "Security-constrained optimal power and natural-gas flow," *IEEE Trans. Power Syst.*, vol. 29, no. 4, pp. 1780–1787, Jul. 2014.

- [8] C. M. Correa-Posada and P. Sánchez-Martín, "Integrated power and natural gas model for energy adequacy in short-term operation," *IEEE Trans. Power Syst.*, vol. 30, no. 6, pp. 3347–3355, Nov. 2015.
- [9] A. Alabdulwahab, A. Abusorrah, X. Zhang, and M. Shahidehpour, "Coordination of interdependent natural gas and electricity infrastructures for firming the variability of wind energy in stochastic day-ahead scheduling," *IEEE Trans. Sustain. Energy*, vol. 6, no. 2, pp. 606–615, Apr. 2015.
- [10] P. Biskas, N. Kanelakis, A. Papamatthaiou, and I. Alexandridis, "Coupled optimization of electricity and natural gas systems using augmented Lagrangian and an alternating minimization method," *Int. J. Elect. Power Energy Syst.*, vol. 80, pp. 202–218, Sep. 2016.
- [11] G. Li, R. Zhang, T. Jiang, H. Chen, L. Bai, and X. Li, "Security-constrained bi-level economic dispatch model for integrated natural gas and electricity systems considering wind power and power-to-gas process," *Appl. Energy*, vol. 194, pp. 696–704, May 2017.
- [12] B. Zhao, A. J. Conejo, and R. Sioshansi, "Unit commitment under gassupply uncertainty and gas-price variability," *IEEE Trans. Power Syst.*, vol. 32, no. 3, pp. 2394–2405, May 2017.
- [13] A. Zlotnik, L. Roald, S. Backhaus, M. Chertkov, and G. Andersson, "Coordinated scheduling for interdependent electric power and natural gas infrastructures," *IEEE Trans. Power Syst.*, vol. 32, no. 1, pp. 600–610, Jan. 2017.
- [14] R. Chen, J. Wang, and H. Sun, "Clearing and pricing for coordinated gas and electricity day-ahead markets considering wind power uncertainty," *IEEE Trans. Power Syst.*, vol. 33, no. 3, pp. 2496–2508, May 2018.
- [15] C. Ordoudis, S. Delikaraoglou, P. Pinson, and J. Kazempour, "Exploiting flexibility in coupled electricity and natural gas markets: A price-based approach," in *Proc. IEEE Manchester PowerTech*, 2017, pp. 1–6.
- [16] M. Gil, P. Dueñas, and J. Reneses, "Electricity and natural gas interdependency: Comparison of two methodologies for coupling large market models within the European regulatory framework," *IEEE Trans. Power Syst.*, vol. 31, no. 1, pp. 361–369, Jan. 2016.

- [17] Y. Chen, W. Wei, F. Liu, and S. Mei, "A multi-lateral trading model for coupled gas-heat-power energy networks," *Appl. Energy*, vol. 200, pp. 180–191, Aug. 2017.
- [18] C. Wang, W. Wei, J. Wang, L. Wu, and Y. Liang, "Equilibrium of interdependent gas and electricity markets with marginal price based bilateral energy trading," *IEEE Trans. Power Syst.*, vol. 33, no. 5, pp. 4854-4867, Sep. 2018.
- [19] Z. Ji and X. Huang, "Coordinated bidding strategy in synchronized electricity and natural gas markets," in *Proc. Asian Conf. Energy, Power, Transp. Electrific.*, 2017, pp. 1–6.
- [20] Z. Ji and X. Huang, "Day-ahead schedule and equilibrium for the coupled electricity and natural gas markets," *IEEE Access*, vol. 6, pp. 27530–27540, 2018
- [21] B. Zhao, A. Zlotnik, A. J. Conejo, R. Sioshansi, and A. M. Rudkevich, "Shadow price-based co-ordination of natural gas and electric power systems," *IEEE Trans. Power Syst.*, vol. 34, no. 3, pp. 1942–1954, May 2019.
- [22] C. B. Sánchez, R. Bent, S. Backhaus, S. Blumsack, H. Hijazi, and P. Van Hentenryck, "Convex optimization for joint expansion planning of natural gas and power systems," in *Proc. 49th Hawaii Int. Conf. Syst. Sci.*, 2016, pp. 2536–2545.
- [23] G. Byeon and P. Van Hentenryck, "Benders subproblem decomposition for discrete-continuous bilevel problems," submitted for publication.
- [24] S. Misra, M. W. Fisher, S. Backhaus, R. Bent, M. Chertkov, and F. Pan, "Optimal compression in natural gas networks: A geometric programming approach," *IEEE Trans. Control Netw. Syst.*, vol. 2, no. 1, pp. 47–56, Mar. 2015.
- [25] G. Morales-España, J. M. Latorre, and A. Ramos, "Tight and compact MILP formulation for the thermal unit commitment problem," *IEEE Trans. Power Syst.*, vol. 28, no. 4, pp. 4897–4908, Nov. 2013.
- [26] C. Borraz-Sánchez, R. Bent, S. Backhaus, H. Hijazi, and P. V. Hentenryck, "Convex relaxations for gas expansion planning," *Informs J. Comput.*, vol. 28, no. 4, pp. 645–656, 2016.
- [27] M. Fischetti, D. Salvagnin, and A. Zanette, "A note on the selection of benders cuts," *Math. Program.*, vol. 124, no. 1-2, pp. 175–182, 2010.
- [28] M. Fischetti, I. Ljubic, and M. Sinnl, "Redesigning benders decomposition for large-scale facility location," *Manage. Sci.*, vol. 63, pp. 2146–2146, 2017
- [29] E. H. Allen, J. H. Lang, and M. D. Ilic, "A combined equivalenced-electric, economic, and market representation of the northeastern power coordinating council U.S. electric power system," *IEEE Trans. Power Syst.*, vol. 23, no. 3, pp. 896–906, Aug. 2008.
- [30] E. Krall, M. Higgins, and R. P. O'Neill, "RTO unit commitment test system," Federal Energy Regulatory Commission, Washington, DC, USA, 2012.
- [31] P. C. A. T. Steven Levine, 'Understanding natural gas markets,' 2014. [Online]. Available: https://www.api.org/media/Files/Oil-and-Natural-Gas/Natural-Gas/API-Understanding-Natural-Gas-Markets.pdf

- [32] "Ruling in docket RM13-17-000," FERC, Washington, DC, USA, 2013.
- [33] V. M. Zavala, K. Kim, M. Anitescu, and J. Birge, "A stochastic electricity market clearing formulation with consistent pricing properties," *Oper. Res.*, vol. 65, no. 3, pp. 557–576, 2017.
- [34] G. Zakeri, G. Pritchard, M. Bjorndal, and E. Bjorndal, "Pricing wind: A revenue adequate, cost recovering uniform price auction for electricity markets with intermittent generation," *Informs J. Optim.*, vol. 1, no. 1, pp. 35–48, 2018.
- [35] A. Philpott, M. Ferris, and R. Wets, "Equilibrium, uncertainty and risk in hydro-thermal electricity systems," *Math. Program.*, vol. 157, no. 2, pp. 483–513, 2016.
- [36] G. Pritchard, G. Zakeri, and A. Philpott, "A single-settlement, energy-only electric power market for unpredictable and intermittent participants," *Oper. Res.*, vol. 58, no. 4-part-2, pp. 1210–1219, 2010.
- [37] J. M. Morales, M. Zugno, S. Pineda, and P. Pinson, "Electricity market clearing with improved scheduling of stochastic production," *Eur. J. Oper. Res.*, vol. 235, no. 3, pp. 765–774, 2014.
- [38] M. Ehrgott, Multicriteria Optimization, vol. 491. Berlin, Germany: Springer, 2005.

Geunyeong Byeon received the B.S. degree from Korea University, Seoul, South Korea and the M.S. degree from Seoul National University, Seoul, South Korea, both in industrial engineering. She is currently working toward the Ph.D. degree with the Department of Industrial and Operations Engineering, University of Michigan, Ann Arbor, MI, USA. Her research interests include operations research with applications in complex, interconnected infrastructure systems.

Pascal Van Hentenryck is the A. Russell Chandler III Chair, and a Professor with the H. Milton Stewart School of Industrial and Systems Engineering, Georgia Institute of Technology, Atlanta, GA, USA. He was a Professor of Computer Science, Brown University for 20 years, the leader of the Optimization Research Group, National ICT Australia (about 70 people), and the Seth Bonder Collegiate Professor with the University of Michigan. He is an INFORMS Fellow and a fellow of the Association for the Advancement of Artificial Intelligence (AAAI). Several of his optimization systems, including OPL and CHIP, have been in commercial use for more than 20 years. His current research interests include artificial intelligence and operations research with applications in energy systems, transportation, resilience, and privacy.